Beyond conformational control: effects of noncovalent interactions on molecular electronic properties of conjugated polymers

Bin Liu,[†] Dario Rocca,[‡] He Yan,[¶] and Ding Pan[*,†,¶,§]

†*Department of Physics, Hong Kong University of Science and Technology, Hong Kong, China*

‡*Université de Lorraine & CNRS, Laboratoire de Physique et Chimie Théoriques (LPCT), F-54000 Nancy, France*

¶*Department of Chemistry, The Hong Kong University of Science and Technology, Hong Kong, China*

§*HKUST Fok Ying Tung Research Institute, Guangzhou, China*

E-mail: dingpan@ust.hk

Abstract

Tuning the electronic properties of polymers is of great importance in designing highly efficient organic solar cells. Noncovalent intramolecular interactions have been often used as conformational control to enhance the planarity of polymers or molecules, which may reduce band gaps and promote charge transfer. However, it is little known if noncovalent interactions may alter the electronic properties of conjugated polymers through some mechanism other than the conformational control. Here, we studied the effects of various noncovalent interactions, including sulfur-nitrogen, sulfur-oxygen, sulfur-fluorine, oxygen-nitrogen, oxygen-fluorine, and nitrogen-fluorine, on the electronic properties of polymers with planar geometry using unconstrained and constrained

density functional theory. We found that the sulfur-nitrogen intramolecular interaction may reduce the band gaps of polymers and enhance the charge transfer more obviously than other noncovalent interactions. Our findings are also consistent with the experimental data. For the first time, our study shows that the sulfur-nitrogen noncovalent interaction may further affect the electronic structure of coplanar conjugated polymers, which cannot be only explained by the enhancement of molecular planarity. Our work suggests a new mechanism to manipulate the electronic properties of polymers to design high-performance small-molecule-polymer and all-polymer solar cells.

Keywords: Noncovalent interactions, conjugated polymers, resonance effect, hole transfer, constrained density functional theory

Introduction

Organic solar cells (OSCs), which consist of heterojunctions of electron-donating and electron-accepting organic matters, have many promising properties; for example, they are inexpensive, environmentally friendly, lightweight, and flexible.[1–5] Recently, substantial progress in designing and synthesizing small-molecule-polymer solar cells, in which the electron donors are conjugated polymers, and the acceptors are non-fullerene small molecules, has boosted the power conversion efficiency up to about 18%.[4,6–11] All-polymer solar cells, where conjugated polymers work as both electron donors and acceptors, also show a promising efficiency of nearly 16%.[12,13] In molecular engineering of small-molecule-polymer or all-polymer solar cells, polymers must be carefully designed, so that electron donors and acceptors can match well.[2] Tens of thousands of donor-acceptor combinations are available, but the scientific community still largely relies on the trial-and-error approach.[5] Many fundamental electronic properties of polymers are not well understood.

Tuning the electronic properties of conjugated polymers plays an important role in optimizing the performance of OSCs. The widely used designing strategies include donor-acceptor copolymers,[2,3,14] fluorination,[15–18] and planar conformation locking.[19–21] In partic-

ular, the high planarity of backbone chains of polymers facilitates electron delocalization and π-π intermolecular interactions, which result in narrower HOMO-LUMO band gaps and fast charge transfer.[3,20] A promising approach of improving the planarity and rigidity of organic molecules is to introduce some noncovalent interactions such as sulfur-nitrogen, sulfur-oxygen, and sulfur-fluorine interactions.[19,21–24] Yu et al. introduced the sulfur-nitrogen interaction as a noncovalent conformational lock in a small molecular acceptor to significantly enhance the photovoltaic performance.[23] Xia et al. found that the sulfur-oxygen interaction has the similar effects in the donor-acceptor conjugated polymers.[22] Some theoretical studies also suggested that noncovalent interactions may enhance planarity of both conjugated polymers and small molecule acceptors.[19,25] So far, most of previous studies focus on how noncovalent interactions control the conformation of polymers, which may further alter electronic properties; however, it is not yet known if noncovalent interactions may directly affect the electronic properties of planar polymers.

In this study, we considered six common noncovalent interactions: sulfur-nitrogen (S-N), sulfur-oxygen (S-O), sulfur-fluorine (S-F), oxygen-nitrogen (O-N), oxygen-fluorine (O-F), and nitrogen-fluorine (N-F), in 48 polymer structures with planar geometry. We found that after introducing the six noncovalent intramolecular interactions, the band gaps of most polymers decrease and the hole transfer rates increase; particularly the sulfur-nitrogen interaction has the most obvious effect. Our findings are also consistent with the experimental data. This study paves the way for understanding and manipulating the electronic properties of polymers, which will facilitate the design of high-performance organic solar cells.

Results and discussion

Figure 1(a) shows the representative structures of conjugated polymers with the six noncovalent interactions. To compare the structures with and without the six noncovalent interactions, we rotated the corresponding moieties around the inter-ring carbon-carbon bonds

by 180° or swapped the side chains (see Figure 1(a) and Figure S1). Before and after the modification, we relaxed both atomic positions and the lengths of repeating units, and found that all the polymers have planar and rigid backbone geometries. The distances of the six noncovalent pairs are smaller than the sum of the van der Waals radii of the corresponding atoms,[26,27] so the noncovalent interactions likely stabilize the polymer structures, which are consistent with previous studies.[21] After we broke up the six noncovalent interactions, the sulfur, nitrogen, oxygen, and fluorine atoms form hydrogen bonds to keep the planar geometry of polymers.

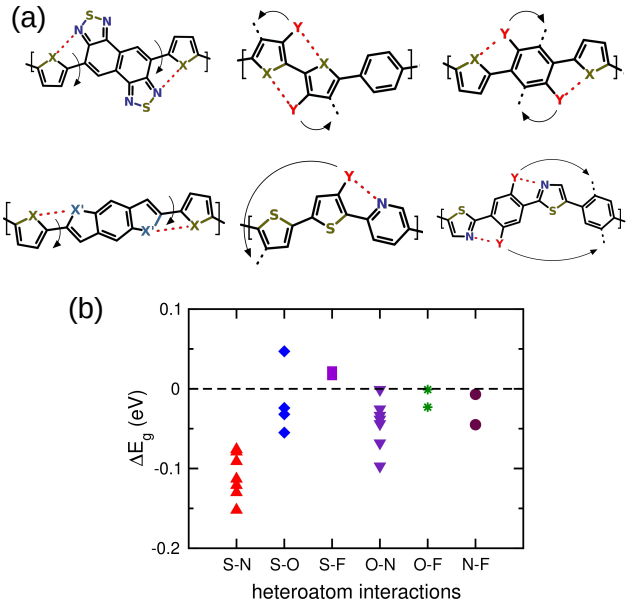

Figure 1: Polymer structures and band gap change. (a) The planar polymer structures with the noncovalent interactions labelled by the dashed lines: S-N, S-O, S-F, O-N, O-F, and N-F. X or X' denotes the S or O atom, and Y is the F atom or the -OCH_3 group. The arrows show that we break up the noncovalent interactions by rotating moieties by 180° or swapping side chains. After the structure modification, the S, N, O, F atoms form hydrogen bonds to keep the planar structures. (b) The change of band gaps after introducing the six noncovalent interactions in (a).

We calculated the electronic structure of the polymers. Figure 1(b) shows the change of HOMO-LUMO band gaps, ΔE_g , after introducing the six noncovalent interactions. We found that the ΔE_g values are largely negative, among which the sulfur-nitrogen interaction reduces band gaps most. The sulfur atom is in the thiophene moiety, and the nitrogen

atom is from benzothiadiazole. We studied seven different polymer structures with the sulfur-nitrogen interaction (see Figures S2 and S3 in the supporting information), whose ΔE_g can be as low as -0.15 eV. In our calculations, we used the vacuum energy level to align the HOMO and LUMO levels, and found that after introducing the sulfur-nitrogen interaction, the HOMO levels shift to higher energies, while the LUMO levels change little (see Figure S5 in the supporting information). Figure 2(a) and (b) show that the HOMO is distributed closer to the polymer backbone than the LUMO, which means that the sulfur-nitrogen interaction may affect the electronic state of the polymer backbone. We plotted the projected density of states of conjugated carbon atoms in Figure 2 (c) and (d), showing that the HOMO is the π bonding orbital, made by the p_z orbitals of the conjugated carbon atoms. The change of the π bonding orbital along the backbone carbon atoms may affect transport properties of polymers.

We calculated the change of hole transfer rates of the polymers after introducing the noncovalent interactions in Figure 3. Because polymers are often used as electron donors in the OSC devices, we mainly consider the hole transport in the hopping regime along the backbone chains. We applied the following adiabatic rate equation:[20,28]

$$k^{Troisi} = \frac{\omega}{2\pi}\left[1 - \exp\left(\frac{-2\pi^{3/2}|H_{AB}|^2}{\hbar\omega\sqrt{\lambda k_B T}}\right)\right] \cdot \exp\left[-\frac{\lambda}{4k_B T} + \frac{|H_{AB}|}{k_B T}\right], \quad (1)$$

where ω is the representative frequency for optical phonons (1000 cm^{-1}), H_{AB} is the non-adiabatic electronic couplings between the A and B states, λ is the reorganization energy, k_B is the Boltzmann constant and T is the temperature (298.15 K). We applied the constrained density functional theory (DFT) method to calculate H_{AB} along the backbone chains.[29] Constrained DFT considers the effects of polarization and orbital relaxation, which are commonly found in the OSC applications.[30] We manually localized charges in polymer moieties using the Becke constraint,[31] and tested a few possible hopping pathways (see Figures. S6

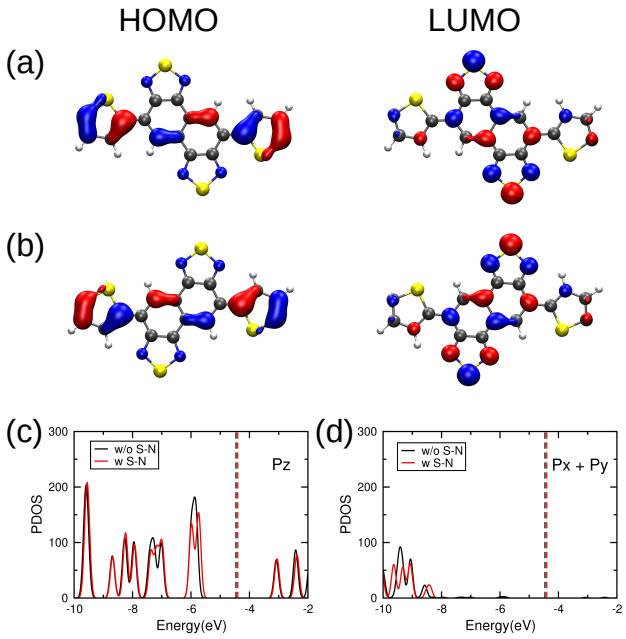

Figure 2: Molecular orbitals and projected densities of states (PDOS) (a) HOMO and LUMO of the polymer NC_{S-N}-1 with the sulfur-nitrogen noncovalent interaction (w S-N). (b) HOMO and LUMO of the polymer HB-1 without the sulfur-nitrogen noncovalent interaction (w/o S-N). (c) PDOS on the p_z orbital of the conjugated carbon atoms in the polymers NC_{S-N}-1 and HB-1. (d) PDOS on the p_x and p_y orbitals of the conjugated carbon atoms in the polymers NC_{S-N}-1 and HB-1. The red and black dashed lines are the Fermi levels in the polymers NC_{S-N}-1 and HB-1, respectively. The energy levels are aligned using the vacuum energy level as the zero energy reference.

and S7). The reorganization energy λ contains two parts:

$$\lambda = \lambda_{in} + \lambda_{ext}. \tag{2}$$

λ_{in} is the internal reorganization energy, and can be calculated as[32]

$$\lambda = E_0(Q_+) - E_0(Q_0) + E_+(Q_0) - E_+(Q_+), \tag{3}$$

where Q_0 and Q_+ correspond to the optimized neutral and cationic polymer structures, respectively, $E_0(Q_+)$ is the energy of the neutral state calculated with the cationic structure, and $E_+(Q_0)$ is the energy of the cationic state calculated with the neutral structure. The external reorganization energy λ_{ext} accounts for the response of surrounding molecules in the charge-transfer process, which is 0.14 eV for all the polymers studied here.[33] While Marcus theory is widely used to calculate the charge hopping rates, because for the polymers studied here the non-adiabatic couplings (H_{AB}) are larger than $\lambda/2$, we applied Eq. (1) instead of Marcus theory.[20,28]

In Figure 3, we compared the hole transfer rates between the two nearest repeating moieties participating in the noncovalent interactions. The sulfur-nitrogen interaction increases the hole transfer rate by $10^2 \sim 10^7$ times, which is overall the largest among all the noncovalent interactions studied here. The results suggest that the sulfur-nitrogen interaction does not only reduce band gaps, but also considerably improve transport properties.

To understand why the sulfur-nitrogen interaction changes band gaps and hole transfer rates most, we first examined the intramolecular charge redistribution using the Mulliken population analysis.[34] We found that after the thiophene sulfur interacts with the pyridinic nitrogen, the sulfur atom loses electrons, while the nitrogen atom gains electrons; the charge redistribution is along the carbon backbone, as shown in Figure 4(a). The intramolecular charge redistribution affects the resonance effect in conjugated polymers, which may help to stabilize the quinoid structure and reduce the band gaps.[35] For example, Figure 4(a) shows

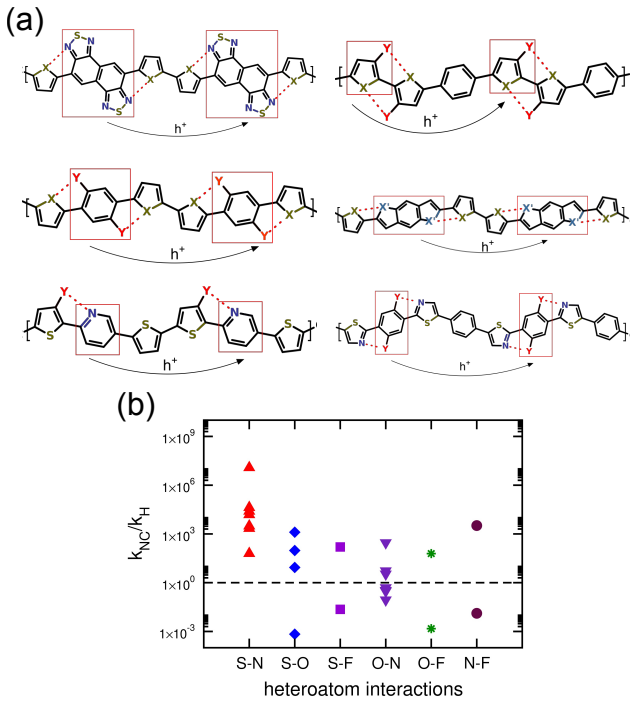

Figure 3: Hole hopping pathways and transfer rates. (a) The pathways show that holes hop from the moieties involved in the noncovalent interactions to the same moieties in the adjoining repeat units in the polymers. (b) The ratio of hole transfer rates (k_{NC}/k_H) between the polymers with and without the noncovalent interactions.

the aromatic and quinoid forms of the polymer NC_{S-N}-1 with the sulfur-nitrogen interaction. The single and double bonds of the thiophene ring in the aromatic structure become the double and single bonds in the quinoid structure, respectively, so the corresponding bond lengths may change if there is more quinoid character. Figure 4 (b) shows the correlation between the bond length change (Δr) and the band gap change (ΔE_g), suggesting that the more quinoid character helps to reduce the band gap, which is consistent with Brédas' findings in polyaromatic molecules.[35] Thus, the sulfur-nitrogen interaction induces the intramolecular charge redistribution in polymers, which increases the quinoid character and reduces the band gaps.

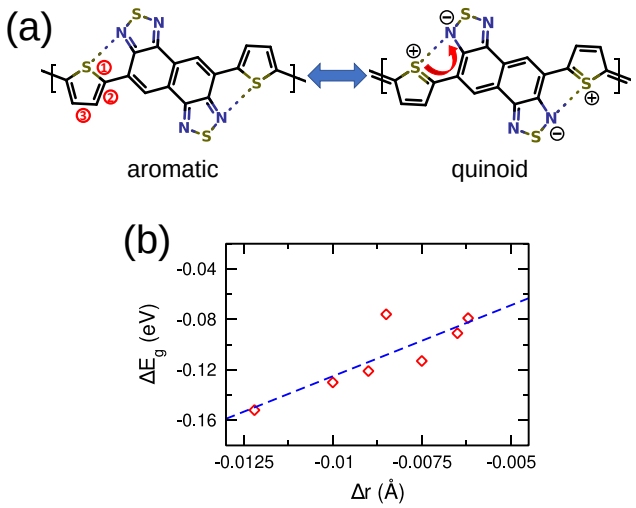

Figure 4: Resonance structures and the decrease of polymer band gaps. (a) Aromatic and quinoid structures of the polymer NC_{S-N}-1 with the sulfur-nitrogen interaction. (b) After the noncovalent interactions form, the change of polymer band gaps, ΔE_g, as a function of Δr. r is calculated as $r = d_{①} - d_{②} + d_{③}$, where $d_{①}$, $d_{②}$, and $d_{③}$ are the S-C, C=C, and C-C bond lengths in the thiophene moiety. The dashed line shows the linear fit.

The sulfur-nitrogen pair has the largest charge redistribution among all the noncovalent interactions studied here (see Table SII in the supporting information), so it affects band gaps and hole transfer rates more than other noncovalent atom pairs. When the thiophene sulfur interacts with the pyridinic nitrogen, the sulfur atom loses about 0.062±0.04 electrons and the nitrogen atom gains about 0.034±0.007 electrons. If we replace the sulfur atom in

the thiophene moiety by the oxygen atom, i.e., thiophene becoming furan (see Figure S4 in the supporting information), the oxygen atom loses about 0.039 $\pm$0.007 electrons and the nitrogen atom may gain as little as 0.010 electrons or even lose 0.022 electrons. The oxygen atom is more electronegative than either the sulfur or the nitrogen atoms, so it is difficult for the oxygen atom to donate electrons to the C-C bonds, which explains why the oxygen-nitrogen pair does not have the similar intramolecular charge redistribution as the sulfur-nitrogen pair. As a result, the quinoid character does not increase obviously with the oxygen-nitrogen interaction, and the band gaps and hole transfer rates do not change much.

For the sulfur-oxygen interaction, when the thiophene sulfur interacts with the benzodifuran oxygen, the quinoid character changes little, so it changes band gaps and hole transport rates little. When the fluorine atom interacts with the sulfur, nitrogen, or oxygen atoms as shown in Figure 1, the fluorine atom may increase the planarity of polymers and enhance the charge separation; however, it does not increase the quinoid character, so the noncovalent interactions with the fluorine atom change electronic properties little.

The Mulliken population analysis largely depends on basis sets, so can only provide estimated partial atomic charges. We also performed the Löwdin population analysis,[36] and found that despite different charge values, both methods give the consistent charge transfer direction (see Table SII in the supporting information).

The effects of noncovalent interactions on the photovoltaic performance of polymers can be also found in experiment. Liu et al. reported that two planar polymers, P3TEA and P3TAE, differ only by the position of carboxyl side chains (see Figure 5(a) and (b)), but have different electronic properties and OSC performance.[37] Our DFT calculations show that the band gap of P3TEA is smaller than that of P3TAE by 0.08 eV, which is consistent with the experimental optical gap change ($\sim$0.05 eV).[37] Additionally, when a hole hops between two nearest 5,6-difluoro-2,1,3-benzothiadiazole (ffBT) moieties, the calculated transfer rate of P3TEA is larger than that of P3TAE by 10^6 times. When Liu et al. blended P3TEA with various molecular acceptors to make OSC devices, its narrower gap and faster charge

transfer lead to the high photovoltaic performance.[37–40] Both P3TEA and P3TAE have the sulfur-nitrogen interaction, except that the carboxyl side chain in P3TAE is next to the sulfur-nitrogen pair. The Mulliken population analysis in Figure 5(c) shows that the pyridinic nitrogen atom in P3TAE becomes less negatively charged than that in P3TEA by about 0.02 e due to the presence of the oxygen atom, so the quinoid character of P3TAE backbone increases less than that of P3TEA, which explains why P3TAE has a larger band gap and worse OSC performance.

(a)

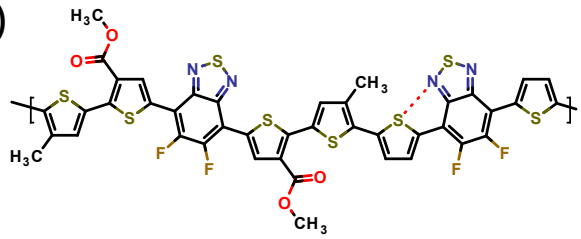

P3TEA

(b)

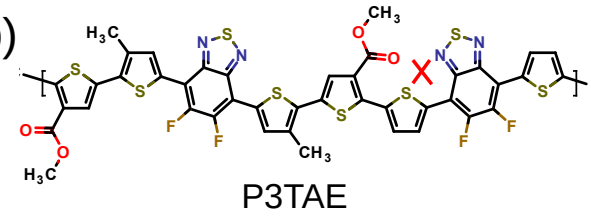

P3TAE

(c)

	Mulliken atomic charge (e)	
Polymer	Thiophene-S	Pyridinic-N
P3TEA	0.982	-0.447
P3TAE	1.144	-0.425

Figure 5: Structures of the polymers (a) P3TEA and (b) P3TAE. (c) Mulliken atomic charges of the thiophene sulfur atom and the pyridinic nitrogen atom in P3TEA and P3TAE.

Conclusion

Here, we applied the unconstrained and constrained DFT method to study six noncovalent intramolecular interactions typically found in the polymers in organic solar cell applications.

Besides conformational control, we found that most of the noncolvalent interactions reduce the band gaps of polymers and increase the hole transfer rates, and the sulfur-nitrogen pair has the largest effect, which cannot be only explained by the enhancement of molecular planarity. The enhancement of electronic properties can be attributed to the intramolecular charge redistribution, which increases the quinoid character of conjugated polymers. Our findings are also consistent with the experimental data. Our study suggests that choosing suitable noncovalent intramolecular interactions may further manipulate the electronic properties of planar polymers. This work paves the way for understanding the electronic structure of polymers, and suggests a new mechanism to design high-performance polymers for small-molecule-polymer and all-polymer solar cells. This mechanism can be also used to improve the performance of organic field-effect transistors.

Method

We conducted first-principles calculations using the Quickstep module of the CP2K program package with a dual basis of Gaussian orbitals and plane waves.[41] We used the Goedecker-Teter-Hutter norm-conserving pseudopotentials for the valence electrons.[42,43] A plane-wave density cutoff of 600 Ry was adopted. We used 3-dimensional periodic boundary conditions to simulate polymers, whose backbone chains are along the z direction. The length of repeating units was obtained by optimizing the structure of dimers and trimers with open boundary conditions.[20] The vacuum along the x and y directions is at least 20 Å thick. We applied the molecularly optimized Gaussian basis sets of double zeta plus polarization quality (DZVP-MOLOPT)[44] and the Perdew-Burke-Ernzerhof (PBE)[45] exchange-correlation (xc) functional with Grimme's D3 dispersion correction[46] in the structural relaxation, where the force tolerance is 0.01 eV/Å. In the band gap calculations, we used Gaussian basis sets of triple zeta plus two sets of polarization functions (TZV2P) and the hybrid B3LYP xc functional.[47–49] In the charge transfer calculations, we used the auxiliary density matrix

method (ADMM)[50] and the cFIT3 basis set to reduce computational costs of the B3LYP functional.

Acknowledgement

D.R. and D.P. acknowledge the financial support by a grant from the PROCORE-France/Hong Kong Joint Research Scheme sponsored by the Research Grants Council of Hong Kong and the Consulate General of France in Hong Kong (Reference Nos. 46911XA and F-HKUST603/20). D.R. acknowledges financial support through the COMETE project (COnception in silico de Materiaux pour l'EnvironnemenT et l'Energie) co-funded by the European Union under the program "FEDER-FSE Lorraine et Massif des Vosges 2014-2020". D.P. acknowledges support from the Croucher Foundation through the Croucher Innovation Award, National Natural Science Foundation of China through the Excellent Young Scientists Fund, and the Energy Institute in Hong Kong University of Science and Technology.

Supporting Information Available

The Supporting Information is available free of charge.

- Polymer structures, HOMO and LUMO levels, non-adiabatic electronic couplings, reorganization energies, hole hopping rates, and change of Mulliken atomic charges and Löwdin atomic charges.

References

(1) Günes, S.; Neugebauer, H.; Sariciftci, N. S. Conjugated polymer-based organic solar cells. *Chem. Rev.* **2007**, *107*, 1324–1338.

(2) Lu, L.; Zheng, T.; Wu, Q.; Schneider, A. M.; Zhao, D.; Yu, L. Recent advances in bulk heterojunction polymer solar cells. *Chem. Rev.* **2015**, *115*, 12666–12731.

(3) Liu, C.; Wang, K.; Gong, X.; Heeger, A. J. Low bandgap semiconducting polymers for polymeric photovoltaics. *Chem. Soc. Rev.* **2016**, *45*, 4825–4846.

(4) Zhang, G.; Zhao, J.; Chow, P. C.; Jiang, K.; Zhang, J.; Zhu, Z.; Zhang, J.; Huang, F.; Yan, H. Nonfullerene acceptor molecules for bulk heterojunction organic solar cells. *Chem. Rev.* **2018**, *118*, 3447–3507.

(5) Zhang, J.; Tan, H. S.; Guo, X.; Facchetti, A.; Yan, H. Material insights and challenges for non-fullerene organic solar cells based on small molecular acceptors. *Nat. Energy* **2018**, *3*, 720–731.

(6) Yuan, J.; Zhang, Y.; Zhou, L.; Zhang, G.; Yip, H.-L.; Lau, T.-K.; Lu, X.; Zhu, C.; Peng, H.; Johnson, P. A., et al. Single-junction organic solar cell with over 15% efficiency using fused-ring acceptor with electron-deficient core. *Joule* **2019**, *3*, 1140–1151.

(7) Liu, S.; Yuan, J.; Deng, W.; Luo, M.; Xie, Y.; Liang, Q.; Zou, Y.; He, Z.; Wu, H.; Cao, Y. High-efficiency organic solar cells with low non-radiative recombination loss and low energetic disorder. *Nat. Photonics.* **2020**, *14*, 300–305.

(8) Zhu, C.; Yuan, J.; Cai, F.; Meng, L.; Zhang, H.; Chen, H.; Li, J.; Qiu, B.; Peng, H.; Chen, S., et al. Tuning the electron-deficient core of a non-fullerene acceptor to achieve over 17% efficiency in a single-junction organic solar cell. *Energy Environ. Sci.* **2020**, *13*, 2459–2466.

(9) Li, S.; Li, C.-Z.; Shi, M.; Chen, H. New Phase for Organic Solar Cell Research: Emergence of Y-Series Electron Acceptors and Their Perspectives. *ACS Energy Lett.* **2020**, *5*, 1554–1567.

(10) Cui, Y.; Yao, H.; Hong, L.; Zhang, T.; Tang, Y.; Lin, B.; Xian, K.; Gao, B.; An, C.; Bi, P., et al. Organic photovoltaic cell with 17% efficiency and superior processability. *Natl. Sci. Rev.* **2020**, *7*, 1239–1246.

(11) Liu, Q.; Jiang, Y.; Jin, K.; Qin, J.; Xu, J.; Li, W.; Xiong, J.; Liu, J.; Xiao, Z.; Sun, K., et al. 18% Efficiency organic solar cells. *Sci. Bull.* **2020**, *65*, 272–275.

(12) Jia, T.; Zhang, J.; Zhang, K.; Tang, H.; Dong, S.; Tan, C.-H.; Wang, X.; Huang, F. All-polymer solar cells with efficiency approaching 16% enabled using a dithieno [3', 2': 3, 4; 2", 3": 5, 6] benzo [1, 2-c][1, 2, 5] thiadiazole (fDTBT)-based polymer donor. *J. Mater. Chem. A.* **2021**, *9*, 8975–8983.

(13) Ma, R. et al. All-polymer solar cells with over 16% efficiency and enhanced stability enabled by compatible solvent and polymer additives. *Aggregate* **2021**, e58.

(14) Holliday, S.; Li, Y.; Luscombe, C. K. Recent advances in high performance donor-acceptor polymers for organic photovoltaics. *Prog. Polym. Sci.* **2017**, *70*, 34–51.

(15) Son, H. J.; Wang, W.; Xu, T.; Liang, Y.; Wu, Y.; Li, G.; Yu, L. Synthesis of fluorinated polythienothiophene-co-benzodithiophenes and effect of fluorination on the photovoltaic properties. *J. Am. Chem. Soc.* **2011**, *133*, 1885–1894.

(16) Stuart, A. C.; Tumbleston, J. R.; Zhou, H.; Li, W.; Liu, S.; Ade, H.; You, W. Fluorine substituents reduce charge recombination and drive structure and morphology development in polymer solar cells. *J. Am. Chem. Soc.* **2013**, *135*, 1806–1815.

(17) Leclerc, N.; Chávez, P.; Ibraikulov, O. A.; Heiser, T.; Lévêque, P. Impact of backbone fluorination on π-conjugated polymers in organic photovoltaic devices: a review. *Polymers* **2016**, *8*, 11.

(18) Zhang, Q.; Kelly, M. A.; Bauer, N.; You, W. The curious case of fluorination of conjugated polymers for solar cells. *Acc. Chem. Res.* **2017**, *50*, 2401–2409.

(19) Jackson, N. E.; Savoie, B. M.; Kohlstedt, K. L.; Olvera de la Cruz, M.; Schatz, G. C.; Chen, L. X.; Ratner, M. A. Controlling conformations of conjugated polymers and small molecules: The role of nonbonding interactions. *J. Am. Chem. Soc.* **2013**, *135*, 10475–10483.

(20) Goldey, M. B.; Reid, D.; de Pablo, J.; Galli, G. Planarity and multiple components promote organic photovoltaic efficiency by improving electronic transport. *Phys. Chem. Chem. Phys.* **2016**, *18*, 31388–31399.

(21) Huang, H.; Yang, L.; Facchetti, A.; Marks, T. J. Organic and Polymeric Semiconductors Enhanced by Noncovalent Conformational Locks. *Chem. Rev.* **2017**, *117*, 10291–10318.

(22) Xia, B.; Lu, K.; Yuan, L.; Zhang, J.; Zhu, L.; Zhu, X.; Deng, D.; Li, H.; Wei, Z. A conformational locking strategy in linked-acceptor type polymers for organic solar cells. *Polym. Chem.* **2016**, *7*, 1323–1329.

(23) Yu, S.; Chen, Y.; Yang, L.; Ye, P.; Wu, J.; Yu, J.; Zhang, S.; Gao, Y.; Huang, H. Significant enhancement of photovoltaic performance through introducing S...N conformational locks. *J. Mater. Chem. A.* **2017**, *5*, 21674–21678.

(24) Li, S.; Zhao, W.; Zhang, J.; Liu, X.; Zheng, Z.; He, C.; Xu, B.; Wei, Z.; Hou, J. Influence of Covalent and Noncovalent Backbone Rigidification Strategies on the Aggregation Structures of a Wide-Band-Gap Polymer for Photovoltaic Cells. *Chem. Mater.* **2020**, *32*, 1993–2003.

(25) Mahmood, A.; Tang, A.; Wang, X.; Zhou, E. First-principles theoretical designing of planar non-fullerene small molecular acceptors for organic solar cells: manipulation of noncovalent interactions. *Phys. Chem. Chem. Phys.* **2019**, *21*, 2128–2139.

(26) Bondi, A. van der Waals volumes and radii. *J. Phys. Chem.* **1964**, *68*, 441–451.

(27) Welch, G. C.; Bakus, R. C.; Teat, S. J.; Bazan, G. C. Impact of regiochemistry and isoelectronic bridgehead substitution on the molecular shape and bulk organization of narrow bandgap chromophores. *J. Am. Chem. Soc.* **2013**, *135*, 2298–2305.

(28) Troisi, A. Charge transport in high mobility molecular semiconductors: Classical models and new theories. *Chem. Soc. Rev.* **2011**, *40*, 2347–2358.

(29) Holmberg, N.; Laasonen, K. Efficient constrained density functional theory implementation for simulation of condensed phase electron transfer reactions. *J. Chem. Theory Comput.* **2017**, *13*, 587–601.

(30) Kaduk, B.; Kowalczyk, T.; Van Voorhis, T. Constrained density functional theory. *Chem. Rev.* **2012**, *112*, 321–370.

(31) Becke, A. D. A multicenter numerical integration scheme for polyatomic molecules. *J. Chem. Phys* **1988**, *88*, 2547–2553.

(32) Brédas, J.-L.; Beljonne, D.; Coropceanu, V.; Cornil, J. Charge-transfer and energy-transfer processes in π-conjugated oligomers and polymers: a molecular picture. *Chem. Rev.* **2004**, *104*, 4971–5004.

(33) Cheung, D. L.; Troisi, A. Theoretical study of the organic photovoltaic electron acceptor PCBM: Morphology, electronic structure, and charge localization. *J. Phys. Chem. C.* **2010**, *114*, 20479–20488.

(34) Mulliken, R. S. Electronic population analysis on LCAO–MO molecular wave functions. I. *J. Chem. Phys.* **1955**, *23*, 1833–1840.

(35) Brédas, J. L. Relationship between band gap and bond length alternation in organic conjugated polymers. *J. Chem. Phys.* **1985**, *82*, 3808–3811.

(36) Löwdin, P.-O. On the non-orthogonality problem connected with the use of atomic wave

functions in the theory of molecules and crystals. *The Journal of Chemical Physics* **1950**, *18*, 365–375.

(37) Liu, J.; Ma, L.-K.; Sheong, F. K.; Zhang, L.; Hu, H.; Zhang, J.-X.; Zhang, J.; Li, Z.; Ma, C.; Han, X., et al. Carboxylate substitution position influencing polymer properties and enabling non-fullerene organic solar cells with high open circuit voltage and low voltage loss. *J. Mater. Chem. A.* **2018**, *6*, 16874–16881.

(38) Liu, J.; Chen, S.; Qian, D.; Gautam, B.; Yang, G.; Zhao, J.; Bergqvist, J.; Zhang, F.; Ma, W.; Ade, H., et al. Fast charge separation in a non-fullerene organic solar cell with a small driving force. *Nat. Energy* **2016**, *1*, 1–7.

(39) Zhang, J.; Li, Y.; Huang, J.; Hu, H.; Zhang, G.; Ma, T.; Chow, P. C.; Ade, H.; Pan, D.; Yan, H. Ring-fusion of perylene diimide acceptor enabling efficient nonfullerene organic solar cells with a small voltage loss. *J. Am. Chem. Soc.* **2017**, *139*, 16092–16095.

(40) Zhang, J.; Bai, F.; Li, Y.; Hu, H.; Liu, B.; Zou, X.; Yu, H.; Huang, J.; Pan, D.; Ade, H., et al. Intramolecular π-stacked perylene-diimide acceptors for non-fullerene organic solar cells. *J. Mater. Chem. A.* **2019**, *7*, 8136–8143.

(41) VandeVondele, J.; Krack, M.; Mohamed, F.; Parrinello, M.; Chassaing, T.; Hutter, J. Quickstep: Fast and accurate density functional calculations using a mixed Gaussian and plane waves approach. *Comput. Phys. Commun.* **2005**, *167*, 103–128.

(42) Krack, M. Pseudopotentials for H to Kr optimized for gradient-corrected exchange-correlation functionals. *Theor. Chem. Acc.* **2005**, *114*, 145–152.

(43) Genovese, L.; Deutsch, T.; Neelov, A.; Goedecker, S.; Beylkin, G. Efficient solution of Poisson's equation with free boundary conditions. *J. Chem. Phys.* **2006**, *125*, 074105.

(44) VandeVondele, J.; Hutter, J. Gaussian basis sets for accurate calculations on molecular systems in gas and condensed phases. *J. Chem. Phys.* **2007**, *127*, 114105.

(45) Perdew, J. P.; Burke, K.; Ernzerhof, M. Generalized Gradient Approximation Made Simple. *Phys. Rev. Lett.* **1996**, *77*, 3865–3868.

(46) Grimme, S.; Antony, J.; Ehrlich, S.; Krieg, H. A consistent and accurate ab initio parametrization of density functional dispersion correction (DFT-D) for the 94 elements H-Pu. *J. Chem. Phys.* **2010**, *132*, 154104.

(47) Becke, A. D. A new mixing of Hartree–Fock and local density-functional theories. *J. Chem. Phys.* **1993**, *98*, 1372–1377.

(48) Stephens, P. J.; Devlin, F. J.; Chabalowski, C. F.; Frisch, M. J. Ab Initio Calculation of Vibrational Absorption and Circular Dichroism Spectra Using Density Functional Force Fields. *J. Phys. Chem.* **1994**, *98*, 11623–11627.

(49) Lee, C.; Yang, W.; Parr, R. G. Development of the Colle-Salvetti correlation-energy formula into a functional of the electron density. *Phys. Rev. B.* **1988**, *37*, 785–789.

(50) Guidon, M.; Hutter, J.; VandeVondele, J. Auxiliary density matrix methods for Hartree-Fock exchange calculations. *J. Chem. Theory Comput* **2010**, *6*, 2348–2364.

TOC Graphic

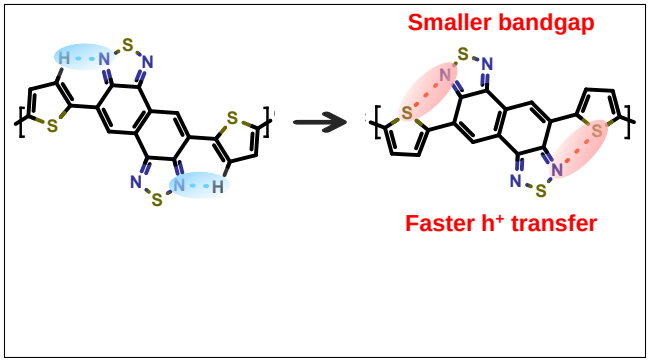

Supporting information: Beyond conformational control: effects of noncovalent interactions on molecular electronic properties of conjugated polymers

Bin Liu,[†,‖] Dario Rocca,[†] He Yan,[‡] and Ding Pan[*,¶]

†*Université de Lorraine & CNRS, Laboratoire de Physique et Chimie Théoriques (LPCT), F-54000 Nancy, France*

‡*Department of Chemistry, The Hong Kong University of Science and Technology, Hong Kong, China*

¶*Department of Physics, Hong Kong University of Science and Technology, Hong Kong, China*

§*HKUST Fok Ying Tung Research Institute, Guangzhou, China*

‖*Department of Physics, Hong Kong University of Science and Technology, Hong Kong, China*

E-mail: dingpan@ust.hk

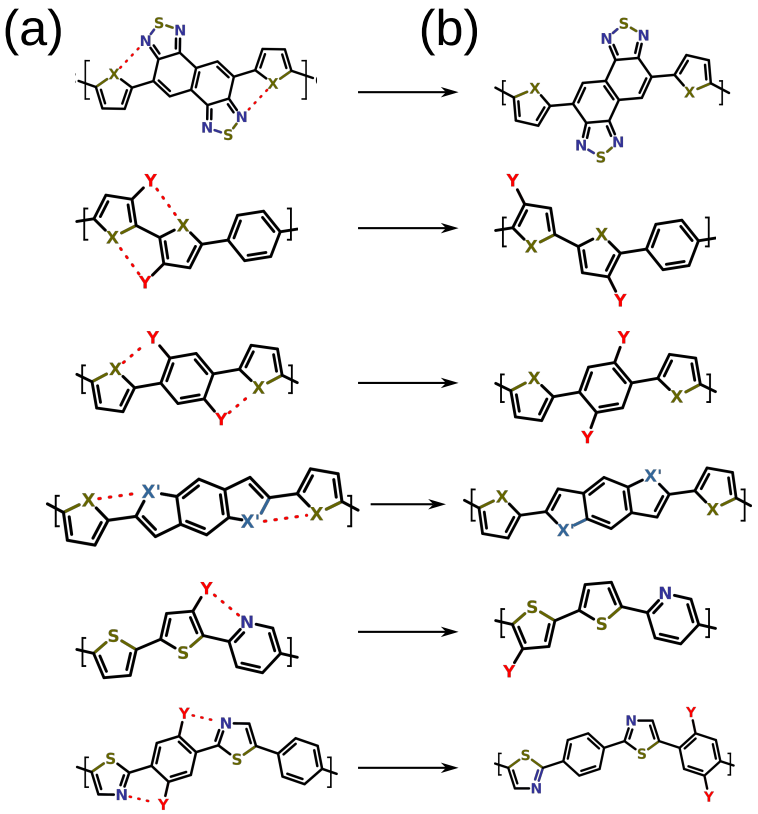

Figure S1: Polymer structures (a) with and (b) without the S-N, S-O, S-F, O-N, O-F, and N-F noncovalent interactions (dashed lines). X or X' are the S or O atom, and Y is the F atom or the -OCH_3 group. We break up the noncovalent interactions by rotating moieties by 180° or swapping side chains. The S, N, O, F atoms form hydrogen bonds in the polymers in (b). All the polymers have the planar structure.

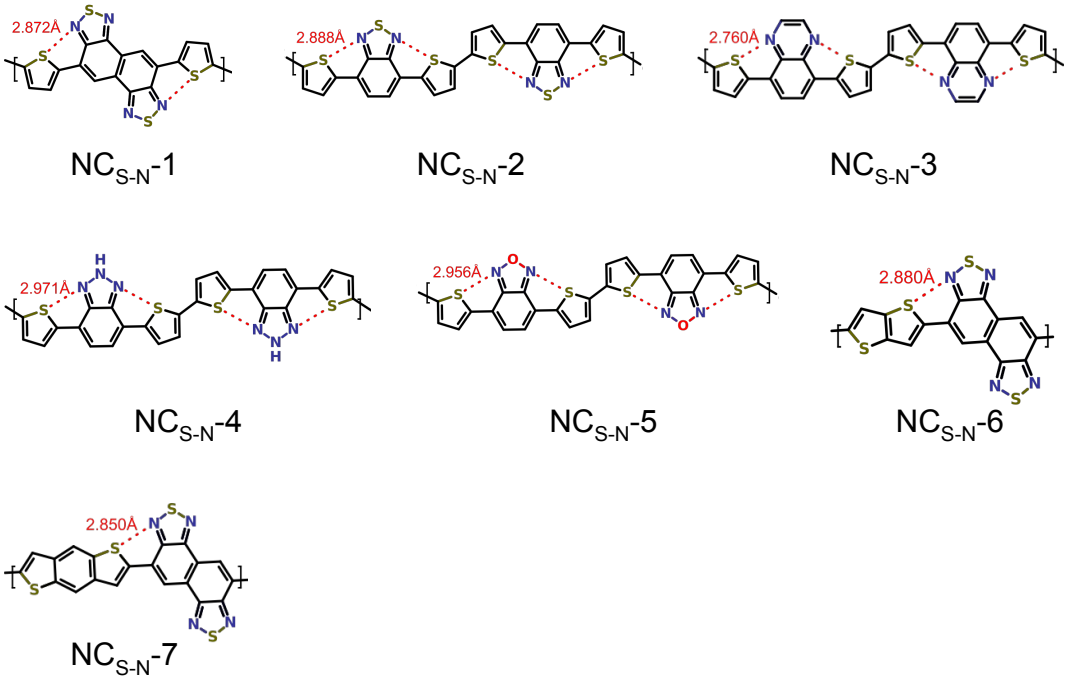

Figure S2: Seven polymer structures with the sulfur-nitrogen interaction.

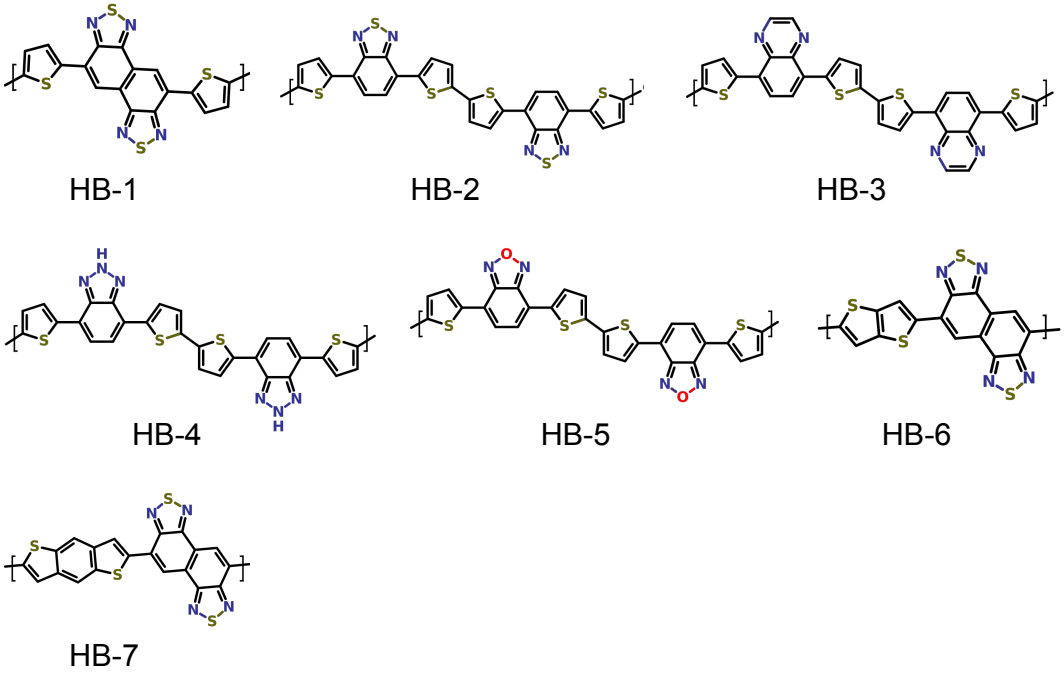

Figure S3: Seven polymer structures without the sulfur-nitrogen interaction obtained by rotating the moieties or swapping the side chains in the structures in Fig. S2. The S and N atoms form hydrogen bonds to keep the planar geometry of polymers.

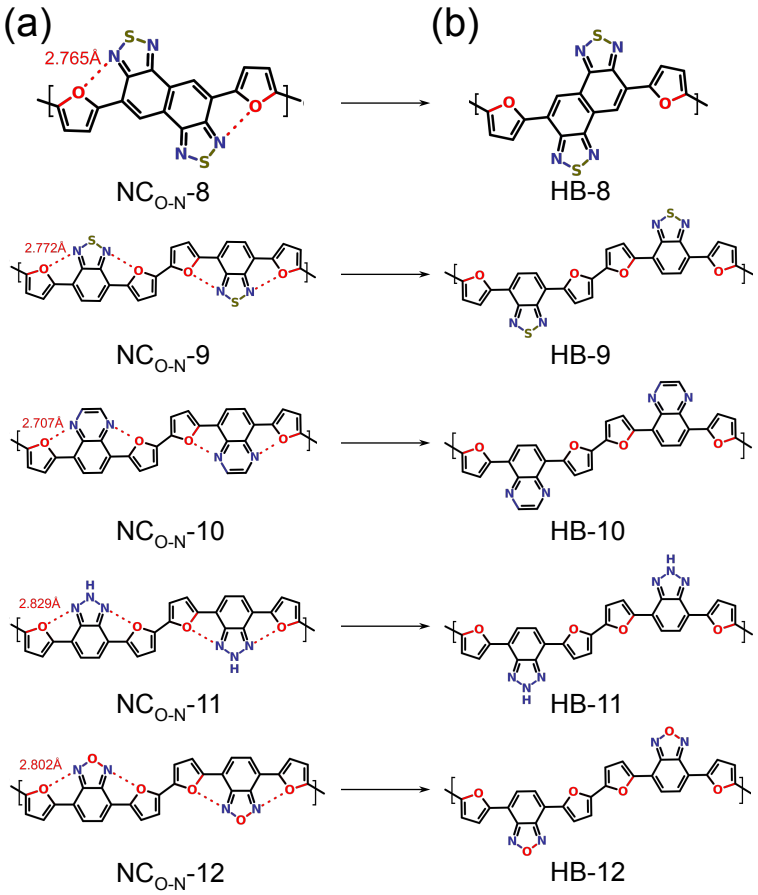

Figure S4: Polymer structures (a) with and (b) without the oxygen-nitrogen interaction. The O and N atoms form hydrogen bonds to keep the planar geometry of polymers.

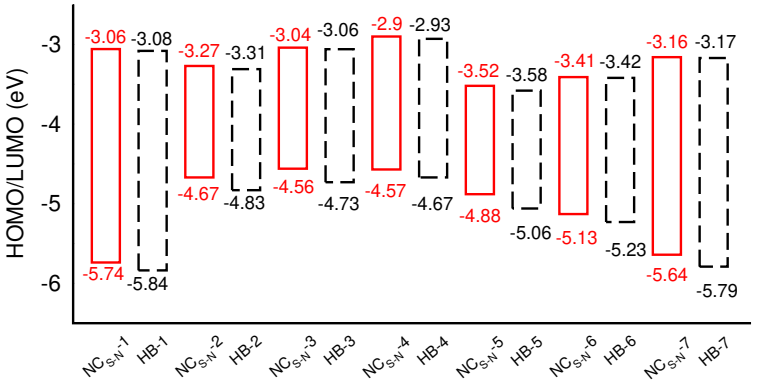

Figure S5: HOMO and LUMO levels of the polymers with and without the sulfur-nitrogen interaction. The polymer structures are shown in Fig. S2 and S3. The energy levels are aligned using the vacuum energy level as the zero energy reference.

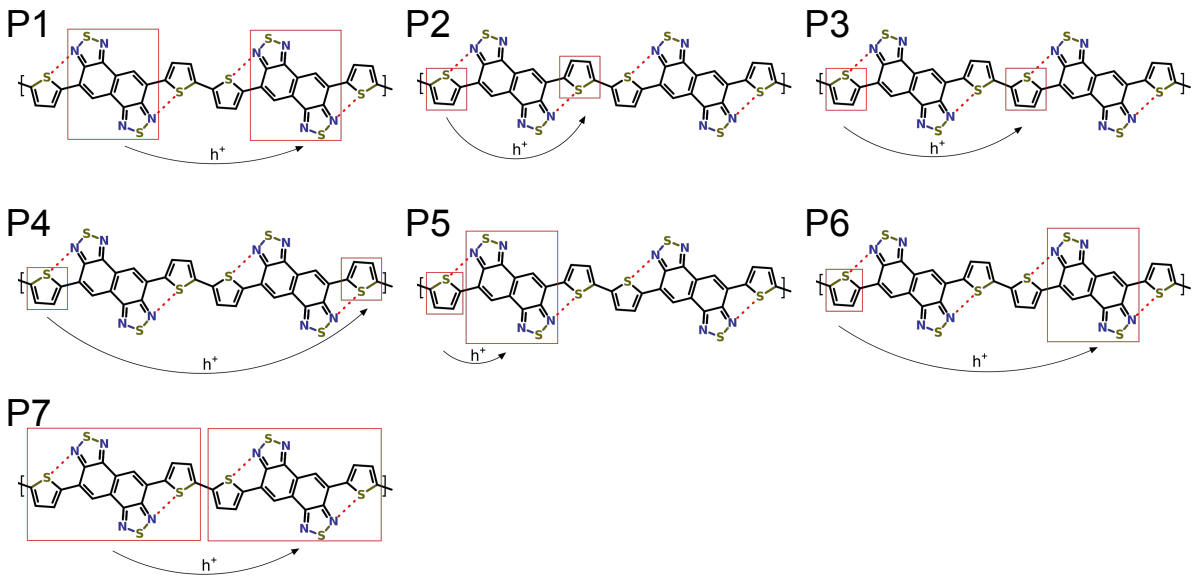

Polymer	Hopping Pathway P1	P2	P3	P4	P5	P6	P7
NC_{S-N}-1	2.12	2.20	2.05	4.38	3.32	2.36	1.98
HB-1	1.83	2.07	1.95	4.35	3.25	2.16	1.78
NC_{S-N}-2	2.56	2.44	2.19	4.14	3.81	2.61	1.85
HB-2	2.30	2.31	2.08	4.12	3.82	2.45	1.73
NC_{S-N}-3	2.84	2.32	2.09	4.13	3.80	2.67	1.80
HB-3	2.41	2.20	2.00	4.11	3.87	2.49	1.65
NC_{S-N}-4	2.37	2.46	2.22	4.21	4.01	2.63	1.85
HB-4	2.17	2.34	2.11	4.17	3.94	2.44	1.75
NC_{S-N}-5	2.68	2.41	2.16	4.09	3.87	2.65	1.81
HB-5	2.44	2.31	2.07	4.08	3.88	2.49	1.74

Figure S6: Non-adiabatic electronic couplings , H_{AB}, of seven hopping pathways in the polymers with ((NC_{S-N}-1 $\sim$ NC_{S-N}-5)) and without (HB-1 $\sim$ HB-5) the sulfur-nitrogen interaction. The unit is eV.

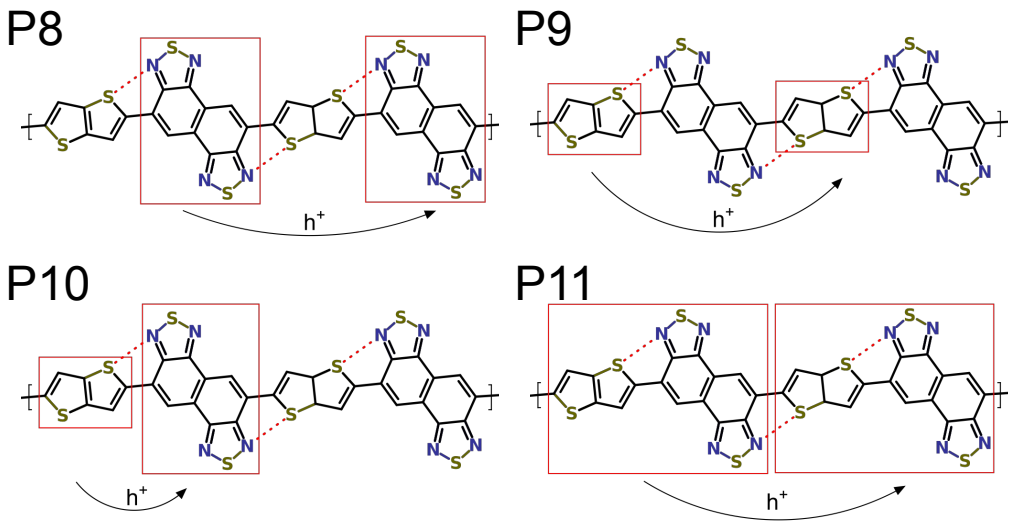

Polymer	Hopping Pathway P8	P9	P10	P11
NC_{S-N}-6	1.88	1.32	2.44	1.57
HB-6	1.75	1.28	2.32	1.52
NC_{S-N}-7	1.76	0.87	1.66	1.21
HB-7	1.55	0.81	1.58	1.19

Figure S7: Non-adiabatic electronic couplings , H_{AB}, of four hopping pathways in the polymers with ((NC_{S-N}-6 and NC_{S-N}-7)) and without (HB-6 and HB-7) the sulfur-nitrogen interaction. The unit is eV.

Table SI: Reorganization energies, λ, and hole hopping rates, k^{Troisi}, obtained by the Troisi rate equation. We compared the pathway P1 for the polymers NC_{S-N}-1 $\sim$ NC_{S-N}-5 and HB-1 $\sim$ HB-5, and the pathway P8 for the polymers NC_{S-N}-6, NC_{S-N}-7, HB-6, and HB-7.

Polymer	$\lambda(eV)$	$k^{Troisi}(s^{-1})$
NC_{S-N}-1	0.47	2.16×10^{47}
HB-1	0.4	5.09×10^{42}
NC_{S-N}-2	0.52	3.75×10^{54}
HB-2	0.49	2.43×10^{50}
NC_{S-N}-3	0.63	6.51×10^{58}
HB-3	0.59	5.41×10^{51}
NC_{S-N}-4	0.54	1.78×10^{51}
HB-4	0.56	5.735×10^{47}
NC_{S-N}-5	0.52	4.44×10^{56}
HB-5	0.57	1.76×10^{52}
NC_{S-N}-6	0.64	3.02×10^{42}
HB-6	0.57	4.8×10^{40}
NC_{S-N}-7	0.36	5.93×10^{41}
HB-7	0.29	2.71×10^{38}

Table SII: Change of Mulliken atomic charges and Löwdin atomic charges after introducing the noncovalent interactions between the atoms X and Y. The positive values mean that the atoms are losing electrons and thus more positively charged.

	Change of Mulliken atomic charge (e)		Change of Löwdin atomic charge (e)	
X-Y	X	Y	X	Y
S-N	0.0616±0.0400	-0.0335±0.0070	0.0314±0.0048	-0.0058±0.0021
S-O	0.0097±0.0744	-0.0089±0.0066	0.0178±0.0097	-0.0067±0.0016
S-F	0.0447±0.0008	0.0047±0.0004	0.0145±0.0068	-0.0045±0.0018
O-N	0.0394±0.0067	0.0062±0.0158	0.0196±0.0018	0.0050±0.0017
O-F	0.0166±0.0030	0.0159±0.0002	0.0061±0.0043	0.0031±0.0010
N-F	0.0420±0.0060	0.0364±0.0023	0.0113±0.0028	0.0181±0.0015